Photoluminescence and positron annihilation spectroscopy of MeV Si^+ ion-irradiated Si_yO_{1-y}:Er ($y \approx 1/3$) thin films

D. E. Blakie,[1] O. H. Y. Zalloum,[1] J. Wojcik,[1] E. A. Irving,[1] A. P. Knights,[1,a)] P. Mascher,[1] and P. J. Simpson[2]
[1]*Department of Engineering Physics, Centre for Emerging Device Technologies, McMaster University, Hamilton, Ontario L8S 4L7, Canada*
[2]*Department of Physics and Astronomy, University of Western Ontario, London N6A 3K7, Canada*

(Received 9 November 2008; accepted 17 January 2009; published online 12 March 2009)

Amorphous erbium-doped silicon oxide (Si_yO_{1-y}:Er, $y \geq 1/3$) thin films are currently under investigation as a luminescent material system for complementary metal-oxide semiconductor compatible light emitters. We have grown films with $y \approx 1/3$ and investigated their properties using both positron annihilation and photoluminescence (PL) spectroscopies. Films were characterized "as deposited," following irradiation with 1 MeV Si^+ ions and after isochronal annealing. The PL yield from both Er^{3+} ions and sensitizing defects is reduced by irradiation, depending strongly on the irradiation fluence and reaching saturation at $\sim 4 \times 10^{13}$ Si^+/cm^2. Higher implantation fluences result in an open-volume defect structure in the film that persists after annealing. This annealing behavior is similar to that of an unrecoverable quenching effect on Er^{3+}-related PL near 1540 nm, and we suggest that these open-volume defects may cause a decoupling of the Er^{3+} ions from sensitizing oxide point defects that form as a result of the film deposition process. © *2009 American Institute of Physics*. [DOI: 10.1063/1.3086644]

I. INTRODUCTION

Erbium-doped silicon rich silicon oxide (Si_yO_{1-y}:Er with $y \geq 1/3$) thin films are currently being investigated as a luminescent material system to fulfill light emission and optical amplification functions for integrated silicon optoelectronic applications.[1] This research is motivated in part by a desire to begin replacing high line-density copper-based electrical interconnect architectures with an optical equivalent in order to meet growing bandwidth demands. Si nanoclusters (Si ncls) embedded in a SiO_2 matrix, formed through the thermally induced phase separation of Si atoms in the oxide network, constitute photoluminescence (PL) centers with broadband aggregate optical emission and absorption properties.[2] While radiative recombination of carriers in a Si ncl can proceed through various channels, excited Si ncls can preferentially couple to nearby Er^{3+} ions,[3] which are introduced as a dopant in the oxide matrix by processes such as cosputtering, ion implantation, or metalorganic chemical vapor deposition. This coupling enables nonradiative energy transfer from an excited Si ncl to Er^{3+} ions, which ultimately relax by the emission of characteristic luminescence near 1540 nm through one of the various radiative transitions from the $^4I_{13/2}$ manifold to the $^4I_{15/2}$ (ground) manifold. Because it has proven difficult to incorporate this sensitization process in electroluminescent devices, much work is still ongoing to elucidate all of the luminescence mechanisms in this material.

The present work investigates the effect of oxide defects on the sensitization mechanism by subjecting an Er-doped oxide film deposited by electron cyclotron resonance plasma enhanced chemical vapor deposition (ECR-PECVD) to a damaging irradiation with a high energy Si^+ ion beam and examining the effect on the film luminescence and defect properties. It is well known that such ion bombardment of insulating thin films produces various electronic/charged defects through inelastic scattering of incident ions from bound target electrons while target vacancies are produced by elastic scattering between nuclei in the target and the incident ion. PL spectroscopy and Doppler broadening detected positron annihilation spectroscopy (PAS) with a variable energy slow positron beam were used to characterize the effect of the irradiation and subsequent recovery through stepwise isochronal annealing. The PAS results are presented in terms of the *S* (or *W*) parameter. The *S* parameter provides an indication of the relative number of positron annihilation events which take place with target core and valence electrons. Positrons which are trapped at defect sites experience an electron environment different from those which annihilate with the unirradiated bulk, and hence a semiquantitative determination of the type and concentration of defects may be acquired by comparison of the *S* (or *W*) parameter of an irradiated sample and that not subjected to ion implantation.

Previous studies which investigated the damaging of silicon oxide thin films by ion irradiation focused on Si-rich compositions only;[4,5] consideration of the impact on the PL properties was typically restricted to the characteristic emission from Si ncls. Following Ar^+ irradiation, Brusa *et al.*[6] found that thermal treatment at 500 °C removed electronic defects in the oxide but vacancy defects were still detectable (by Doppler broadening PAS) in the substrate after annealing at 1100 °C and in the oxide in the case of high excess Si content. Alternatively, Hirata *et al.*[7] used PAS to measure the *S* parameter in SiO_2 films on *c*-Si following implantation

a)Author to whom correspondence should be addressed. Electronic mail: aknight@mcmaster.ca.

with 30 keV Er^+ ions. Considering ion fluences of 3.0×10^{14} and 1.5×10^{15} cm^{-2}, it was found that the *S* parameter increased with postimplant annealing up to 900 °C but was always much higher in the sample receiving the lower implant fluence; in neither case the preimplant *S* parameter value was recovered. The decrease in the *S* parameter was attributed to severe structural damage of the SiO_2 network, trapping of positrons (thus preventing their evolution to Ps) at Er^{3+} bond sites, or the elimination of Ps formation sites by the bonded Er. Cathodoluminescence measurements showed no Er^{3+} emission near 1540 nm from as-implanted samples; however, an increasingly strong emission was developed following annealing from 600 °C to 900 °C. Interestingly, all defects detectable by electron spin resonance (ESR) measurements, for the sample receiving the higher implant fluence, had disappeared by 600 °C.

Such irradiation studies are relevant for two reasons. First, silicon oxide thin films are often doped by implantation either with Er or with other codopants such as carbon selected to produce particular luminescence emission.[8,9] It is important to understand the effect of such irradiation on the intrinsic luminescence centers of the initial film, as well as those formed by postirradiation annealing. Second, an ability to categorize the basic irradiation-induced defects (such as with PAS) can permit the identification of those classes of defects to which the desired luminescence centers may be sensitive. Based on such an understanding, the tailoring of the film preparation processes to minimize such defects may assist in enhancing the overall efficiency of these materials.

II. EXPERIMENTAL DETAILS

A. Sample preparation and description

A single amorphous Si_yO_{1-y}:Er thin film was deposited on a *p*-type *c*-Si wafer using ECR-PECVD with *in situ* Er doping. The details of the McMaster ECR-PECVD system, as well as the fitting of the system with the *in situ* Er-doping capability, have been described elsewhere.[10,11] The Si precursor was 30% SiH_4 in Ar, the O precursor was 10% O_2 in Ar, and the Er precursor was the metalorganic complex $Er(tmhd)_3$. The volatile Er chelate is heated to generate a small amount of vapor which is then carried by an Ar gas flow from the heating cell to a dispersion ring in the deposition chamber. The film was deposited with a SiH_4 mass flow rate of 20 cubic centimeter per minute at STP (SCCM) and an O_2 flow rate of 64 SCCM. The Er cell temperature was 120 °C and the Ar carrier gas flow rate was fixed at 18 SCCM. The microwave discharge power was 500 W. The chamber pressure was reduced to $\sim 10^{-7}$ Torr prior to deposition; chamber pressure during deposition was ~3 mTorr. The substrate was heated to a temperature of 120 °C prior to and during deposition, and the substrate was rotated at 20 rpm throughout the growth. The film composition, as determined by Rutherford backscattering spectrometry using a 1.5 MeV beam of $^4He^+$ ions, was approximately 33.5 at. % Si relative to O with 1.32 at. % Er relative to Si and O.

Following deposition, the wafer was cleaved into several samples. Each was annealed for 3 h at 800 °C in a Jipelec JetFirst 100 rapid thermal annealer under flowing N_2 gas. This was done to optimize the film luminescence near 1540 nm. Following the measurement of the PL in both spectral ranges of interest (details provided below), the samples were subjected to a damaging irradiation. The irradiation was carried out using a 1.7 MV tandetron accelerator to produce a 1 MeV Si^+ ion beam. Simulations using the program SRIM (Ref. 12) indicated that such ion beam parameters would prevent codoping of the film with Si atoms since the ion range would be greater than 1 μm. Each sample received one irradiation at a fluence of 1×10^{12}, 5×10^{12}, 1×10^{13}, 2×10^{13}, 4×10^{13}, 5×10^{13}, or 1×10^{15} Si^+/cm^2; the beam current was always less than 200 nA and sample heating above room temperature was negligible. Immediately following irradiation, the samples were divided into two groups: first group to be characterized by PAS and the second to undergo stepwise annealing and PL measurements. The annealing schedule used isochronal heating of 10 min duration, carried out under flowing N_2 gas ambient, with a stepwise temperature sequence from 150 to 800 °C in steps of 50°, followed by anneals at 900 and 1000 °C.

B. Laser-excited PL characterization

Room temperature infrared PL spectra were measured from 1400 to 1650 nm. The PL setup consists of a 17 mW He-Cd laser operating at a wavelength of 325 nm, a grating monochromator, a lock-in amplifier with a chopper, and an InGaAs detector. Both the entrance and exit slits for the monochromator were 3 mm. The system response curve is approximately flat over the bandwidth of the Er signal near 1540 nm, and therefore the spectra do not require further correction. Room temperature PL spectra were also measured from 350 to 1000 nm using the same laser but with a rerouted beam. The signal was collected using an S2000 miniature fiber optic spectrometer from Ocean Optics. These latter spectra were fully corrected for the system response and optics transmission. A description of the PL system and data correction methodology is given elsewhere.[13] For the purpose of this study, all PL spectra in the 350–1000 nm band have been converted to normalized photon flux units.

C. Doppler broadening PAS

PAS was carried out using the slow positron beam facility at the University of Western Ontario. A full description of the apparatus has been given elsewhere.[14] A description of the Doppler broadening parameters and positron and positronium physics has also been given elsewhere.[15] The system generates a nearly monoenergetic positron beam from a ^{22}Na source with a thin tungsten transmission moderator. The present study used a beam with variable energy between 0.5 and 33 keV corresponding to mean implanted positron depths in SiO_2 ranging from 5 nm to 4 μm. An intrinsic Ge detector was used to measure the gamma ray energy distributions resulting from the positron annihilation events. All measurements were carried out under high vacuum ($\sim 10^{-7}$ Torr). The *S* and *W* parameters were calculated from the measured spectra for the full range of incident positron energies. In order to provide a measurement standard, spectra were taken for a sample of effectively defect-free single

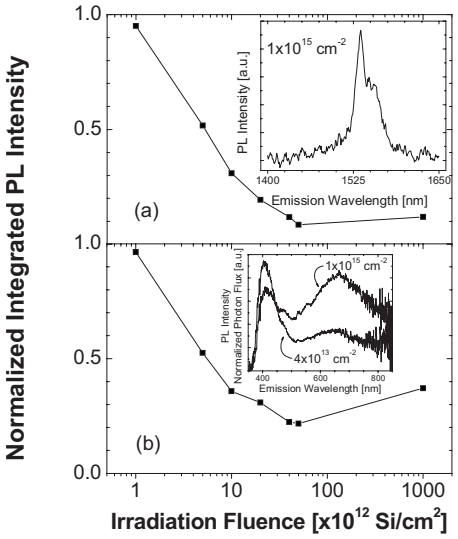

FIG. 1. Integrated PL intensity following irradiation normalized to the value for the unirradiated sample. (a) Infrared wavelength band (1400–1650 nm); (b) visible band (350–850 nm). The inset in (a) shows the raw PL spectrum for the highest irradiation fluence (as-irradiated); the inset in (b) shows the raw PL spectrum for the two highest ion fluences (as-irradiated). All samples were annealed for 3 h at 800 °C in flowing N_2 gas prior to irradiation to optimize the Er-related PL near 1540 nm.

crystal Si. The *S* and *W* parameters presented throughout this report have been normalized to the measured values for undefected bulk Si.

Four samples were selected, immediately following irradiation, for PAS measurements—unirradiated and fluences of 1×10^{13}, 4×10^{13}, and 1×10^{15} Si^+/cm^2. The measurements were conducted at room temperature. Following this, the two samples corresponding to irradiation fluences of 1×10^{13} Si^+/cm^2 and 1×10^{15} Si^+/cm^2 underwent PAS measurements while subject to *in situ* annealing under vacuum. During this measurement, the positron beam energy was fixed near 2 keV (corresponding to a mean positron implant depth in SiO_2 of about 47 nm). For the present study, the temperature was continuously ramped from room temperature to 600 °C over a period of about 5 h.

III. RESULTS AND DISCUSSION

A. PAS and PL in the as-irradiated film

Ion implantation simulations[12] indicate that the concentration of Er vacancy defects caused by the irradiations in this study is small (fewer than 10 at. % of the Er atoms for the highest irradiation fluence). The postirradiation Er-related PL emission should therefore be dominated by electronic damage, particularly defects in the SiO_2 matrix involving dangling bonds such as the E' center, the peroxy radical, and the nonbridging oxygen hole center (NBOHC).[15] As the E' center and peroxy radical are known to be nonradiative, they should constitute pathways for PL quenching; excited Er^{3+} ions will couple strongly to any such defects located in the Er-coordinating shell, leading to fast energy transfers to acceptor states of the defects. Figure 1 depicts the integrated PL intensity obtained from the as-irradiated films. It is believed that the Er-related PL near 1540 nm observed in this

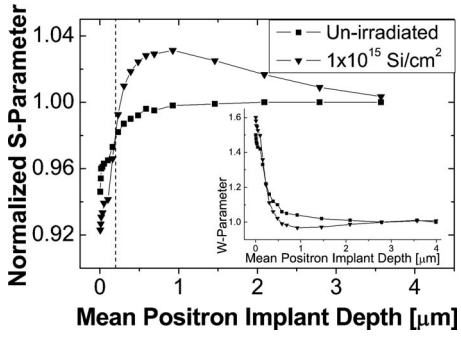

FIG. 2. Positron annihilation *S* parameter and *W* parameter (inset) for both unirradiated and heavily irradiated samples. The dashed line in the main graph indicates the film/substrate interface.

study is potentially sensitized by oxide defects and Si ncl, and that the sensitizing centers emit intrinsic visible PL in the 350–850 nm band.

Figure 1 shows that the PLs in both the infrared (1400–1650 nm) and visible (350–850 nm) bands behave similarly as a function of the irradiation fluence. At the lowest fluence (1×10^{12} Si/cm^2) there is almost no quenching of the PL, which is consistent with the negligibly small concentration of displaced Er atoms predicted by the SRIM simulations. For a fivefold increase in the fluence, the PL is reduced by 50% in both wavelength ranges. However, saturation of the PL quenching sets in between 4×10^{13} and 5×10^{13} Si^+/cm^2, wherein the PL yield will not decrease below about 10% of the preirradiated (maximum) value even if the irradiation fluence is increased 20 fold over this initial *saturation* dose. In fact, in the visible band, there is a slight increase in the integrated intensity. The saturation effect is related to irradiation-induced radiative point defects, such as those which are thought to be intrinsically present in the deposited films, including the weak oxygen bond, the neutral oxygen vacancy, divalent Si, and the NBOHC. For example, at fluences below the saturation value, the introduction of nonradiative defects dominates so that the PL yield decreases. Above the saturation fluence, radiative defects appear in sufficient numbers to compensate the nonradiative centers, preventing further reduction in the PL.

To illustrate the impact of irradiation on the defect population, Fig. 2 shows the positron annihilation *S* and *W* parameters (which have been normalized to the spectrum of the bulk region of defect-free single crystal Si) for the unirradiated samples and for the most heavily irradiated samples studied. The film is only 200 nm thick and so the irradiation changes the *S* and *W* parameters corresponding to both the film and the substrate. Following irradiation, the normalized *S* parameter for the film is decreased below unity. Conversely, irradiation causes an increase in the *S* parameter for the substrate due to the production of vacancylike defects.

The decrease in the *S* parameter within the film, upon irradiation, is attributable to the trapping of positrons at irradiation-induced negatively charged electronic (point) defects, which reduce the probability of Ps formation;[16–18] the fluence is apparently not high enough to form significant voids in the film. In general, the annihilation characteristics of positrons in amorphous silicon oxide films are dominated

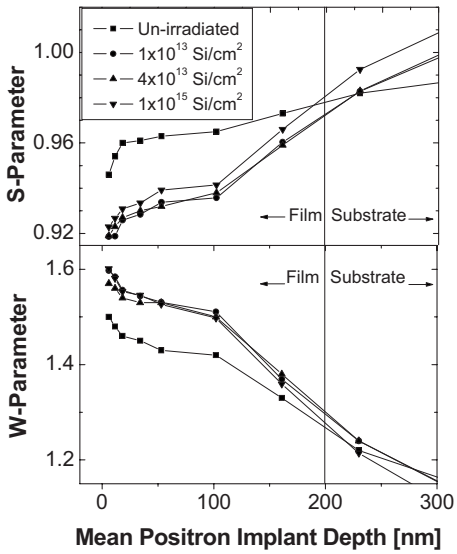

FIG. 3. Positron annihilation *S* parameter (*top*) and *W* parameter (*bottom*) obtained from films subject to various ion fluences.

by Ps formation because almost all implanted positrons annihilate from Ps states.[15] This means that irradiation-induced changes in the *S* parameter *within* the film can usually be explained in terms of changes in Ps formation; in fact, ion irradiation is thought to be able to reduce Ps formation to zero.[16] Note that void space in the films, in which Ps might form, is initially limited in this study because of the long preirradiation anneal at 800 °C. The preanneal should densify the films and release most of the residual hydrogen contamination, thereby reducing irradiation-induced film compaction.[19]

Both the *S* and *W* parameters for the films are plotted in Fig. 3 for various irradiation fluences. The *S* and *W* parameters have apparently saturated even for the sample receiving the lowest irradiation fluence, since there is no further decrease in the *S* parameter for higher fluences. This means that all of the positrons entering the film become trapped before they annihilate and the addition of further trapping defects with higher irradiation fluence has no impact on the value of *S*. This makes the PAS data somewhat difficult to compare with the as-irradiated PL data since the positron saturation occurs at a lower fluence than the PL saturation.

Examination of Fig. 3 reveals that the *S* parameter (and the *W* parameter) within each film shows two different regimes. The first is a knee-shaped region from 0 to 100 nm, while the second is a linear section that extends into the substrate. To look for Ps formation, difference spectra were obtained by subtracting the raw gamma photopeak spectrum of the *c*-Si standard (at a positron energy of ~40 keV) from the spectra of the film specimens such that the positron energy resulted in a mean implantation depth consistent with the first region of the film (~2.5 keV). Figure 4 shows such difference spectra for an unirradiated film and one irradiated to a dose of 1×10^{15} cm^{-2}. The narrow central peak in the difference spectrum can be attributed to the 2-γ annihilation of *p*-Ps.[20] The unirradiated film shows much more Ps formation than the irradiated material.

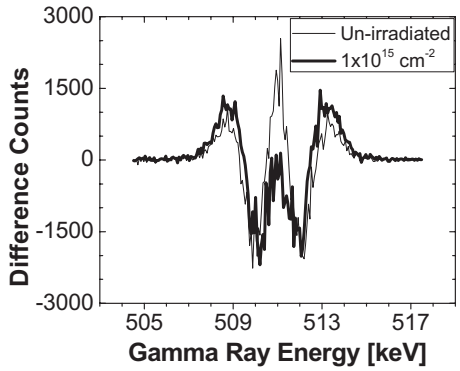

FIG. 4. Difference spectra obtained by subtracting the raw gamma photopeak spectrum of the *c*-Si standard ($E_{\text{positron}}\approx40$ keV) from the spectra of the films under study ($E_{\text{positron}}\approx2.5$ keV). Each spectrum contains 5×10^5 counts.

A possible explanation for the two apparent regimes of the *S* parameter in as-irradiated films is the presence of Er-related positron-trapping defects. It has been suggested[7] that Er^{3+} suppresses Ps formation by trapping positrons and/or occupying spaces where Ps might be formed. The film under study has a nonuniform Er concentration profile, as revealed by the Rutherford backscattering data. In fact, the Er concentration uniformly decreases from a value of 1.7 at. % near the film surface to 0.9 at. % near the substrate, meaning that the region with the most Er is also the region showing an anomaly in the *S* parameter. This could suggest that there is a positron-trapping defect associated with the Er incorporation in these films. We note though that this interpretation is somewhat speculative and complicated by the decreasing resolution of the slow positron technique with increase positron implantation energy.

B. Annealing-induced changes in irradiated films

Figure 5 depicts the recovery of the PL in both spectral bands for two representative samples (implant fluences of 2×10^{13} and 1×10^{15} Si$^+$/cm^2). Parts (a) and (c) show the spectra obtained after annealing at various temperatures, along with the preirradiation PL spectrum. Parts (b) and (d) plot the integrated intensity, normalized to the preirradiation PL yield, as a function of the anneal temperature.

The PL signal in the infrared band shows a monotonic increase in intensity with anneal temperature up to a maximum at 800 °C, beyond which there is a gradual decrease, likely resulting from Er precipitation. The spectral content of the Er^{3+} transition [part (a)] shows no variation with annealing temperature, and the PL intensity recovers almost completely to its preirradiation value following annealing to 800 °C. Although not shown in this figure, annealing at 800 °C for 3 h results in only a marginal increase in the PL over the 10 min anneal. The recovery of the PL follows a smooth trend throughout; it does not show any sharp increases associated with the articulated disappearance of a specific defect at a particular temperature (such as an E' center at 300 °C or a NBOHC at 600 °C).[17] In this sense, the PL does not exhibit sensitivity to any single specific nonradiative defect type. This was true for all of the irradiation fluences studied.

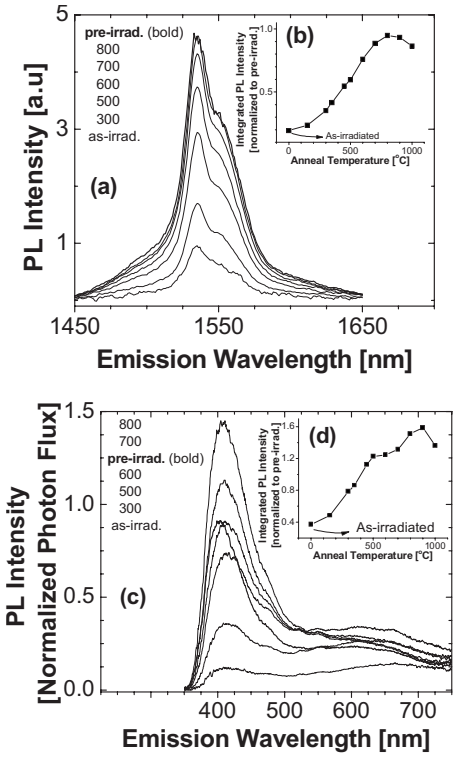

FIG. 5. (Top) Infrared PL spectra and integrated intensities (inset) shown at various anneal temperatures for film irradiated at 2×10^{13} cm^{-2}; (bottom) visible PL spectra and integrated intensities (inset) shown at various anneal temperatures for film irradiated at 1×10^{15} cm^{-2}.

Given that the most common irradiation-induced electronic defects in SiO_2 and Er-doped SiO_2 (i.e., those that are detectable by ESR) are generally repaired by annealing to 600 °C,[17] the fact that the Er^{3+} infrared PL signal is only 76% recovered by 600 °C suggests that there are other defect centers in these films which require a higher temperature to anneal. The destruction of Er-luminescence complexes by the displacement of Er and O during irradiation should not be the main effect since these displacements account for only about 0.5% of the total Er and O populations at an implant fluence of 2×10^{13} Si^+/cm^2. Another consideration is the damage of the sensitizing centers themselves. While studies of Si ncls/nanocrystals that have been damaged by ion irradiation suggest that they can fully recover their luminescent emission at an anneal temperature as low as 800 °C,[5] the film in the present study should contain a small (or even zero) concentration of Si clusters because there is a negligible Si excess. Nonetheless, there are other sensitizing centers in the films, and these must be limiting the Er^{3+} PL. This can be investigated by considering the visible band PL.

The recovery of the visible PL (at a fluence of 1×10^{15} Si^+/cm^2) with annealing, as shown in Fig. 5, follows a much different trend than the infrared PL. For example, the visible PL yield increases steadily with increasing anneal temperature above the as-irradiated value. In fact it recovers 59% *beyond* the preirradiation yield after annealing at 900 °C. There are two notable changes in the spectral content relative to the preirradiation spectrum. The first is the relatively slight redshift of the defect PL peak from 403 nm to 410–415 nm (tentatively ascribed to the weak oxygen bond) following the irradiation, which remains throughout the annealing. This may be due to changes in the dielectric constant of the film (as evidenced by a change in color of the film following irradiation) as a result of the near-complete destruction of the Si-O network. The second is the variation in the ratio of the intensities of the peak centered at 410 nm and the broad feature centered near 600–650 nm. While this ratio is nearly constant between 3 and 4 for the other irradiation fluences (throughout annealing), in this sample it begins at a factor of 0.86 (indicating that the 600–650 nm PL is slightly more intense than the blue-violet PL) in the as-irradiated film and increases to a factor of 6 after annealing to 800 °C, following a smooth trend. This ratio is plotted in Fig. 6 as a function of anneal temperature for irradiation fluences of 1×10^{13} and 1×10^{15} Si^+/cm^2. The broad PL near 650 nm does not recover as quickly as the violet peak, and it decreases in relative intensity beyond 500 °C. This suggests that the defect responsible for the broad feature near 650 nm is related to the NBOHC and is largely repaired at the higher anneal temperatures.

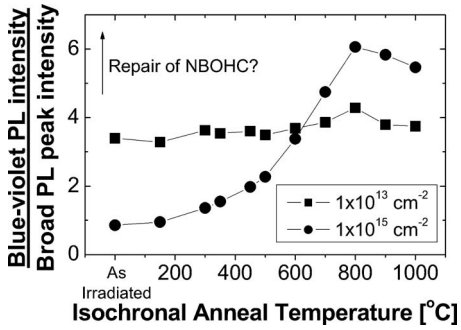

FIG. 6. Ratio of the blue-violet PL peak intensity to that of the broad PL peak centered near 650 nm ($PL_{450\ nm}/PL_{650\ nm}$) as a function of postirradiation anneal temperature for the sample irradiated with a fluence of 1×10^{15} cm^{-2}.

1. Role of the irradiation fluence

Figure 7 compares the recovery of the integrated PL intensity in the infrared and visible bands for various implant fluences. The intensities have been normalized, for each temperature, to the unirradiated control sample which was annealed (and remeasured after each anneal) along with the irradiated samples.

It is clear from Fig. 7 that the trend in the Er^{3+} infrared PL recovery is dependent on the irradiation fluence. For example, the very slight reduction in the PL intensity in the sample irradiated with 1×10^{12} Si^+/cm^2 has recovered by 400 °C. The intermediate fluences up to 1×10^{13} cm^{-2} follow similar smooth PL recovery patterns; in these cases, most of the increase in the signal occurs between 300 and 700 °C, with a flattening of the recovery at higher temperatures. The PL eventually recovers very close to the value of the unirradiated control sample for all fluences except the highest irradiation fluence (1×10^{15} Si^+/cm^2). In the latter case, the PL recovers to a maximum of only 61% of the control sample and the required annealing at 1000 °C. Interestingly, while the sample irradiated at 4×10^{13} Si^+/cm^2 ex-

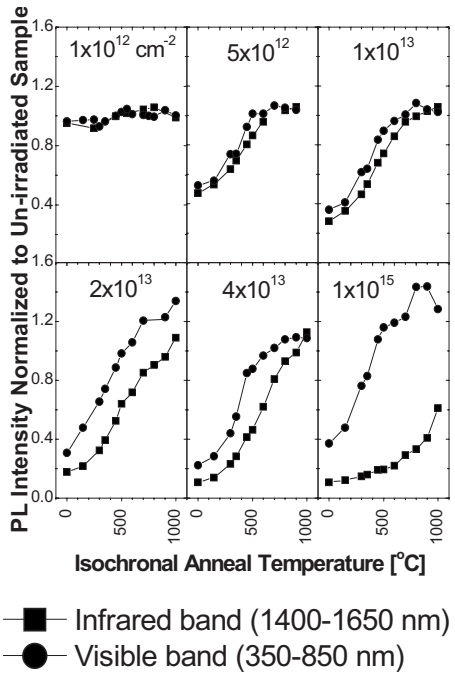

FIG. 7. Integrated PL intensities in both infrared and visible wavelength ranges. Each panel corresponds to a different irradiation fluence. All *y* axes are synchronous.

hibited an initial PL quenching to the same value as the highest fluence, this sample exhibited close to a full recovery.

Comparing the recovery of the infrared band PL to that of the visible band PL, it is apparent that the latter depends less on the fluence. Thus, as the irradiation fluence increases, there is an increase in the difference between the degree of recovery of the PL in the infrared and visible wavelength ranges (i.e., there is a widening of the gap between the two curves). The lowest fluence results in almost no PL quenching and this yield effectively returns to the preirradiated state after a 400 °C anneal. The intermediate fluences all show a fast PL increase up to 500 °C and then a slower increase up to full recovery beyond this. The highest fluence, however, is anomalous yet again, though in a manner that contradicts its behavior in the infrared band. With the exception of this fluence, the similarity of both the annealing trends and shape of the PL recovery curves suggests that the PL near 1540 nm and that near 410 nm must be related. The increasing difference between the PL recovery curves for the infrared Er^{3+} and visible defect PL bands suggests that increasing the irradiation fluence may have the effect of inflicting a progressive decoupling of sensitizing defects (associated with the 410nm band) from the Er^{3+} ions.

The strong PL recovery observed in both wavelength ranges for the intermediate fluences in the 300–700 °C range is consistent with a reduction in defects such as the E' center, peroxy radical, and NBOHC. The continued, though slower, PL recovery in these samples at even higher temperatures suggests that the damaged Er-O complexes are repaired by high temperature annealing. However, this also suggests that there is damage in the film which is still more persistent. Can these defects be identified concurrent with a model in which the Er^{3+} PL is sensitized by radiative defects (other than Si ncl)? The peculiar results obtained for the highest irradiation fluence provide a clue in this regard. Consider that the Er-related PL at 1540 nm is not recoverable by annealing to 1000 °C, while the visible defect PL recovers beyond its preirradiation value. It is tempting to suggest that the irradiation has introduced further radiative electronic defects into the film which result in the observed enhancement of the oxide defect PL. However, this does not seem likely because the spectral shape of the PL in the region of enhancement (350–500 nm) is unchanged. It appears, rather, that the irradiation has allowed a population of defects, which were already present, to emit photons when they were inhibited from doing so before. This could be the set of oxide defects which couple as sensitizers to the Er^{3+} ions. Indeed, there is a 60% reduction in the PL at 1540 nm (relative to the preirradiation PL) for the 900 °C anneal of the 1×10^{15} Si^+/cm^2 fluence. This corresponds with a 60% increase in the visible band PL (relative to the preirradiation PL) in the same sample at the same anneal temperature—which happens to be that at which the defect PL is a maximum. This implies that the enhanced oxide defect PL in the sample receiving the highest irradiation fluence is due to the decoupling of these oxide defects from the Er^{3+} ions, causing a decrease in the Er^{3+} PL at 1540 nm. This would confirm the role of the oxide defects as sensitizers and suggests that as sensitizing defects, they may be unable to emit light when coupled to an Er^{3+} ion. This further suggests that the coupling is very strong, which implies, within the framework of a Förster-Dexter transfer, that the defects must be located close to the Er^{3+} ions. Any observable oxide defect PL must correspond to centers not strongly coupled to an Er^{3+} ion.

It is not obvious why the high fluence irradiation forces a partial decoupling of the Er ions and their sensitizers. It has been previously reported[7] that an Er-doping implant fluence exceeding 1×10^{15} Si^+/cm^2 in a thermal SiO_2 thin film produced a cathodoluminescence quenching at 1.54 μm, which was unrecoverable with annealing. This was ascribed to the presence of persistent defects (not detectable by ESR) resulting from the complete destruction of the SiO_2 network by the high fluence implant to the point where a complete regrowth at 1100 °C would be necessary to repair the structure. Although it was not addressed in that report, one wonders if the reduced PL at the higher irradiation fluence might have been the result of concentration quenching. This explanation may not apply to the films of the present study, however, because it contradicts the extremely strong visible PL being emitted from the films. Figure 7 shows that while the visible PL can indeed be quenched by irradiation-induced electronic defects, it is fully recoverable by annealing at 800–900 °C. On the contrary, as the high irradiation fluence illustrates, the films ultimately yield the same total luminescence, but the relative PL yield in each spectral range shifts to favor blue-violet emission. In other words, the irradiation-induced nonradiative damage is gone but the network itself has been permanently modified. The work of Brusa, *et al.*[6] on Ar^+-irradiated Si-rich SiO_x films suggests that this (persistent) structural modification of the network consists of open-

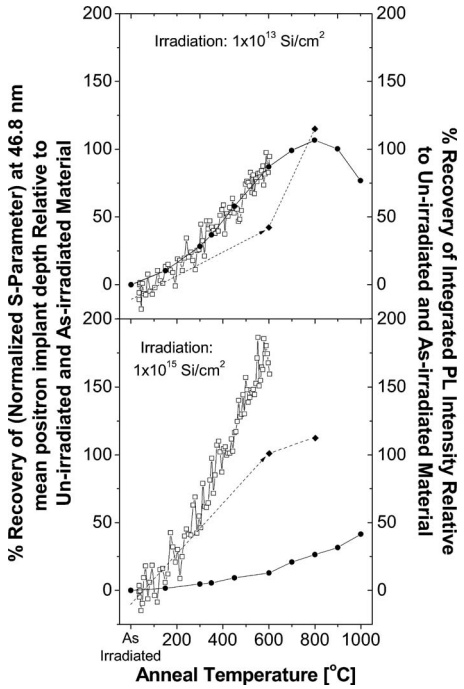

FIG. 8. Integrated infrared PL intensity recovery plotted alongside the positron *S*-parameter recovery as a function of anneal temperature. The upper panel depicts irradiation fluence 1×10^{13} cm^{-2}; the lower panel shows 1×10^{15} cm^{-2}. The dashed line shows the effective *S*-parameter recovery without the effect of the enhanced thermal formation of Ps. Circles—integrated PL intensity (1400–1650 nm band); solid diamond—*S* parameter measured at room temperature following annealing up to the designated temperature; hollow square—*in situ* measurement of *S* parameter during annealing.

volume defects. This could explain why in the present study we only observe the effect of this modification at the highest implant fluence.

2. PAS measurement with in situ annealing

To investigate the possible formation of open-volume defects at the highest irradiation fluence, two samples were annealed *in situ* during positron annihilation measurement. Figure 8 depicts the recovery of the *S* parameter as a function of the instantaneous anneal temperature for irradiation fluences of 1×10^{13} and 1×10^{15} Si^{+}/cm^{2}. These measurements were performed at a constant positron energy of 2 keV, corresponding to a mean depth of ~47 nm, i.e., within the oxide film. The recovery has been expressed as a percentage of the difference between the (normalized) *S* parameter for the as-irradiated and unirradiated samples. Figure 8 also depicts the recovery of the corresponding integrated PL intensity in the 1400–1650 nm band, normalized in the same way as the *S* parameter. The comparison is somewhat indirect since the PL measurements were made at room temperature following annealing and not at elevated temperature.

The *S* value in both samples ultimately underwent a full recovery to that of the unirradiated sample. Before we discuss the correlation of PL yields with the *S* parameters, the effect of temperature on Ps formation must be reviewed.[21,22] The *in situ* measurement of the *S* parameter is complicated by the enhancement of Ps formation (even in the presence of electronic defects) at elevated temperatures, which results from the tendency for thermal detrapping of positrons from electronic defects. This produces an "artificial" enhancement (increase) of the *S* parameter which is not necessarily related to the actual repair of electronic defects. The dashed line in Fig. 8 attempts to portray the "real" *S*-parameter recovery *as it pertains to the recovery of electronic defects*, that is, with Ps thermal effects removed. This is based on the room temperature measurement of the *S* parameter following annealing up to 600 °C. The apparent more rapid rise of the *S* parameter with anneal temperature for the higher fluence sample (and associated total recovery of 190% at high temperatures) is in fact an indication of more Ps formation (both at room temperature and at 600 °C). We conclude then that this sample contains significant open volume compared to the sample subjected to the lower fluence.

The PL at 1540 nm recovers faster than the *S* parameter in the sample receiving the lower fluence of 1×10^{13} cm^{-2}, while it recovers much slower than the *S* parameter in the sample receiving the highest fluence. Given that the Ps formation data in Fig. 8 indicate that the open-volume defect population is the major structural difference between the two films, it seems that the Er^{3+} luminescence is severely quenched by those particular defects. Since these open-volume defects appear to be persistent to 900 °C, the fact that the PL for the sample receiving the lower implant fluence recovered completely means that this sample is likely dominated by electronic defects (which are expected to anneal by 900 °C) with comparatively few defects of a vacancy type. It is difficult to extend the correlation of the PL to any defects other than these. This is because the electronic defects are driving the *S* parameter down while the vacancies are driving the *S* parameter up; the electronic defects and the vacancies do not anneal identically at a given temperature, and the PL near 1540 nm appears to have a particular sensitivity to the vacancies.

The question remains as to whether the vacancylike defects are forcing a decoupling of sensitizer and Er^{3+} PL centers. If this is the case, it remains to be determined how this occurs. It may be related to the decoration of vacancies with other defects or a clustering of Er ions in the vicinity of the vacancies.

IV. CONCLUSIONS

This study investigated the PL centers in Er-doped Si_yO_{1-y} ($y\approx1/3$) thin films deposited by ECR-PECVD with *in situ* Er doping. An analysis has been made of the impact of damaging ion irradiations on the Er^{3+} PL near 1540 nm and the PL from point defect centers responsible for sensitizing Er^{3+} ions. It has emerged that $>1\times10^{12}$ Si^{+}/cm^{2} at 1 MeV is required to produce measurable PL quenching, while a fluence of $\sim4-5\times10^{13}$ Si^{+}/cm^{2} produces a saturation of the PL quenching, at a wavelength of 1540 nm, to a value ~10%–20% of the preirradiation optimized yield. At these fluences, the PAS Doppler broadening *S* and *W* parameters saturate due to the introduction of a large concentration of electronic defects. Increasing the irradiation fluence to 1×10^{15} Si^{+}/cm^{2} initially gives rise to a large number of NBOHC defects and finally results in an apparent decoupling

of the Er^{3+} ions from their sensitizing centers. This is manifested by an enhancement of the PL emission from the sensitizing defects, upon annealing to 800 °C, by 60% beyond the maximum attainable value prior to irradiation; this is accompanied by an unrecoverable quenching of the Er^{3+} PL near 1540 nm. PAS measurements carried out under *in situ* annealing suggest that the main difference between the samples irradiated to $\sim 10^{13}$ Si^+/cm^2 versus 10^{15} Si^+/cm^2 is the predominance of open-volume defects in the latter. While it is not clear that these open-volume defects cause the decoupling of the Er^{3+} ions from their sensitizers, it seems, nonetheless, that the Er^{3+} emission is highly sensitive to the presence of this type of defect.

ACKNOWLEDGMENTS

The authors would like to thank Dr. Willy Lennard and Jack Hendricks from the University of Western Ontario, Canada for their assistance with the ion irradiations and RBS measurements. Jim Garrett of the Brockhouse Institute of Materials Research at McMaster University assisted with annealing facilities. This work was funded by the Canadian Institute for Photonic Innovations (CIPI), the Natural Sciences and Engineering Research Council of Canada (NSERC), and the Ontario Research and Development Challenge Fund (ORDCF) under the auspices of the Ontario Photonics Consortium.

[1] G. T. Reed and A. P. Knights, *Silicon Photonics: An Introduction* (Wiley, New York, 2004).
[2] F. Iacona, C. Bongiorno, C. Spinella, S. Boninelli, and F. Priolo, J. Appl. Phys. **95**, 3723 (2004).
[3] V. Yu. Timoshenko, M. G. Lisachenko, O. A. Shalygina, B. V. Kamenev, D. M. Zhigunov, S. A. Teterukov, P. K. Kashkarov, J. Heitmann, M. Schmidt, and M. Zacharias, J. Appl. Phys. **96**, 2254 (2004).
[4] G. Mariotto, G. Das, A. Quaranta, G. Della Mea, F. Corni, and R. Tonini, J. Appl. Phys. **97**, 113502 (2005).
[5] D. Pacifici, E. C. Moreira, G. Franzò, V. Martorino, F. Priolo, and F. Iacona, Phys. Rev. B **65**, 144109 (2002).
[6] R. S. Brusa, G. P. Karwasz, G. Mariotto, A. Zecca, R. Ferragut, P. Folegati, A. Dupasquier, G. Ottaviani, and R. Tonini, J. Appl. Phys. **94**, 7483 (2003).
[7] K. Hirata, H. Arai, A. Kawasuso, T. Sekiguchi, Y. Kobayashi, and S. Okada, J. Appl. Phys. **90**, 237 (2001).
[8] P. Pellegrino, A. Pérez-Rodriguez, B. Garrido, O. González-Varona, J. R. Morante, S. Marcinkevičius, A. Galeckas, and J. Linnros, Appl. Phys. Lett. **84**, 25 (2004).
[9] C. Barthou, P. H. Duong, A. Oliver, J. C. Cheang-Wong, L. Rodriguez-Fernández, A. Crespo-Sosa, T. Itoh, and P. Lavallard, J. Appl. Phys. **93**, 10110 (2003).
[10] M. Boudreau, M. Boumerzoug, P. Mascher, and P. E. Jessop, Appl. Phys. Lett. **63**, 3014 (1993).
[11] X. D. Pi, O. H. Y. Zalloum, J. Wojcik, A. P. Knights, P. Mascher, A. D. W. Todd, and P. J. Simpson, J. Appl. Phys. **97**, 096108 (2005).
[12] J. F. Ziegler, J. P. Biersack, and U. Littmark, *The Stopping and Range of Ions in Solids* (Pergamon, New York, 1985).
[13] O. H. Y. Zalloum, M. Flynn, T. Roschuk, J. Wojcik, E. A. Irving, and P. Mascher, Rev. Sci. Instrum. **77**, 023907 (2006).
[14] P. J. Schultz, Nucl. Instrum. Methods Phys. Res. B **30**, 94 (1988).
[15] R. Krause-Rehberg, *Positron Annihilation in Semiconductors:Defect Studies* (Springer, Berlin, 2003).
[16] A. Rivera, I. Montilla, A. Alba Garcia, R. Escobar Galindo, C. V. Falub, A. van Veen, H. Schut, J. M. M. de Nijs, and P. Balk, Mater. Sci. Forum **363–365**, 64 (2001).
[17] M. Fujinami and N. B. Chilton, Appl. Phys. Lett. **62**, 1131 (1993).
[18] A. Uedono, T. Kawano, S. Tanigawa, and H. Itoh, J. Phys.: Condens. Matter **6**, 8669 (1994).
[19] S. M. Sze, *VLSI Technology* (McGraw-Hill, New York, 1988).
[20] P. J. Simpson, M. Spooner, H. Xia, and A. P. Knights, J. Appl. Phys. **85**, 1765 (1999).
[21] A. P. Mills, Jr., Phys. Rev. Lett. **41**, 1828 (1978).
[22] P. Sferlazzo, S. Berko, and K. F. Canter, Phys. Rev. B **32**, 6067 (1985).